Site Specific Rotational Mobility of Anhydrous Glucose near the Glass Transition As Studied by 2D Echo Decay ^{13}C NMR

Dagmar van Dusschoten,*,†,‡ Ursula Tracht,† Andreas Heuer,† and Hans W. Spiess†

Laboratory of Molecular Physics, Agricultural University Wageningen, Dreijenlaan 3, 6703 HA Wageningen, The Netherlands, and Max Planck Institut für Polymerforschung, Ackermannweg 10, D-55128 Mainz, Germany

Received: May 25, 1999; In Final Form: August 2, 1999

Site specific ^{13}C labeling of anhydrous glucose is used to study the time scale and geometry of reorientational motion of the exocyclic CH_2OH group in relation to the main glucose ring. By comparison of 2D echo decay NMR experiments with Monte Carlo simulations a bimodal distribution of jump angles, a 75% fraction of 1−2° jumps and a 25% of 7−8° jumps, is found to describe the geometry of the reorientational processes of the main ring. For the CH_2OH group the average jump angle of the larger jump process is somewhat larger. The jump rates for both the CH_2OH group and the ring are similar. The apparent activation energy determined for the rotational motion of the CH_2OH group and the ring is 480 ± 40 kJ/mol, which is very similar to an earlier determination using viscometry. It is concluded that the glucose ring and the exocyclic CH_2OH-group mobility are strongly correlated and that the rotational freedom of the CH_2OH group should not be used to explain the faster β-relaxation process also found for glucose.

Introduction

The nature of the molecular mobility of a supercooled liquid near its glass transition temperature, T_g, is of great interest for understanding the macroscopic changes that are associated with the glass transition.[1,2] In many studies that attempt to determine the nature of molecular mobility near T_g, one resorts to glasses with favorable characteristics, e.g. *o*-terphenyl, toluene, or glycerol.[3,4] However, to better understand the molecular mobility and its relation to macroscopic characteristics in general, it is necessary to make comparisons with other low molecular mass glasses. One group of interesting molecules is provided by the monomeric carbohydrates, which have been extensively studied by differential scanning calorimetry (DSC)[5] and dielectric spectroscopy/relaxation[6−8] and are available in a wide variety with small molecular variations. Most of these carbohydrates consist of a closed ring with hydroxyl groups and an exocyclic group.

The nature of the dynamics and geometry of molecular motion of carbohydrates close to T_g has not been characterized yet. This question, however, is particularly important since it is believed that the exocyclic CH_2OH group, with its additional degrees of freedom, play a major role in the β-relaxation process. This assumption is based on the observation that monomeric sugars without this side group show little or no β-relaxation when studied by dielectric spectroscopy.[7] To investigate this hypothesis, it is therefore essential to know how the relatively small CH_2OH group moves relative to the bigger, main ring. Because of the high specificity of NMR and the ready availability of site-specific ^{13}C labeled glucose, such a hypothesis is open to testing. Even more, not only the time scale of (sub)molecular reorientations can be detected, but using the 2D spin echo decay technique the geometry of the reorientational motion can also be assessed.[9]

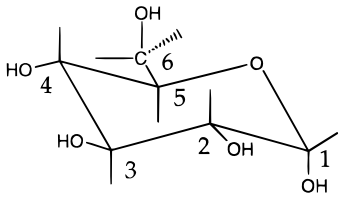

Figure 1. Molecular structure of α-D-glucose. Enantiomerization into β-D-glucose occurs when the hydroxy group at position 1 flips up. ^{13}C enrichment was at position 1 or 6.

α-D-Glucose (Figure 1) is a good candidate for studying molecular mobility in carbohydrates. It is comparable in size with toluene, not as a van der Waals glass but as an H-bridge forming glass, in which respect it is comparable to glycerol, which is also well studied.[3] Compared to glycerol and toluene, anhydrous glucose has a much higher glass transition temperature of 308 K compared to 190 K for glycerol and 117 K for toluene.[10] All three glasses, according to the classifying system developed by Angell,[11] are rather fragile, with toluene having the highest fragility index, $m = 107$, followed by glucose with $m = 79$ and glycerol with $m = 53$.[12] Because of the many hydroxyl groups and the therewith-associated high dipolar moment, glucose, like glycerol, is highly hygroscopic. The presence of water strongly reduces the glass transition temperature, whereby water is thought to cut or destabilize the intraglucose H-bonds.[13]

In recent NMR studies, e.g., refs 9, 10, and 14−16, the reorientational mechanism of deuterated glycerol, toluene, and *o*-terphenyl was studied slightly above their respective calorimetric glass temperatures by using specific multidimensional ^{2}H NMR methods.[17] For glycerol it was concluded that the reorientational mechanism was dominated by small angular jumps of about 2−3° superimposed on a smaller fraction with a 25° average jump angle.[3] Here, we describe similar ^{13}C NMR studies on glucose enriched at the C-1 or C-6 position (see Figure 1) to investigate both molecular and intramolecular

* To whom correspondence should be addressed.
† Current address: Max Planck Institut für Polymerforschung, Ackermannweg 10, D-55128 Mainz, Germany. E-mail: dvd@mpip-mainz.mpg.de.
‡ Agricultural University Wageningen.

10.1021/jp9917244 CCC: $18.00
Published on Web 10/01/1999

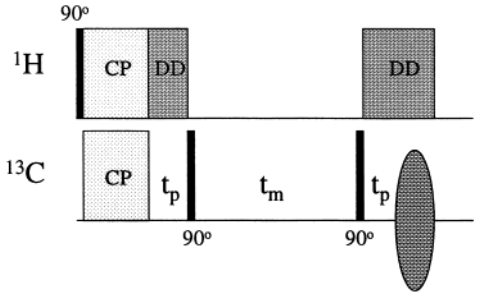

Figure 2. Schematic of the 2D echo decay curve. Here, CP indicates the cross polarization period (typically 1 ms) and DD (during t_p) denotes homo- and hetereonuclear decoupling.

motion in order to see how far the CH_2OH group rotates independently from the main ring.

Experimental Section

A. NMR Experiments. The reorientation of molecules in supercooled viscous liquids can be investigated by measuring a two-time correlation function.[17−19] This correlation function can be obtained by recording different echo signals after a three-pulse excitation. This so-called 2D spin echo decay technique has been described in detail elsewhere,[9,20,21] but for clarity it is briefly summarized here.

In solid-state ^{13}C NMR the frequency of the signal is dependent on the molecular orientation relative to the magnetic field, caused by the anisotropic electron density distribution near the carbon nucleus. The resulting Larmor frequency is expressed as follows[17]

$$\omega(\theta,\phi) = \delta\frac{1}{2}(3\cos^2\theta - 1 - \eta\sin^2\theta\cos(2\phi)) \qquad (1)$$

with δ representing the spectral anisotropy (rad/s) and $0 \le \eta \le 1$ representing the spectral asymmetry, which is small for deuterons. For ^{13}C at the C-1 position in glucose $\delta = 2\pi \times 2.8$ kHz and $\eta = 0.47$, for the carbon at the C-6 position $\delta = 2\pi \times 1.97$ kHz and $\eta = 0.62$ (for a Larmor frequency $\omega = 2\pi.75.47$ MHz). These values were readily obtained from normal solid-state spectra (see, e.g., Schmidt-Rohr and Spiess[17]) of crystalline glucose samples. It is unknown how the chemical shift tensor is aligned relative to the molecular axis for either of these enriched molecules, which, however, is no problem for the subsequent analysis.

For deuterons the two-time correlation function can be obtained by using a simple three-pulse NMR sequence.[20] For ^{13}C, however, it is necessary to use cross-polarization via the protons to maximize the ^{13}C transversal magnetization (see Figure 2). This magnetization evolves with a frequency given by eq 1, until, after a period t_p (the evolution period) the sine or cosine part of the magnetization is stored along the *z*-axis when the second ^{13}C rf pulse is applied. Rotational motion during the following time interval, t_m, or mixing time, causes the isochromats to evolve with a different frequency after application of the third pulse. Isochromats at fixed orientations give rise to an echo, whereas changes of the molecular orientation lead to a reduction of the echo. Depending on the phase of the second rf pulse relative to the first pulse, one either measures the cosine part of the two-time autocorrelation function, as expressed by eq 2a, or the sine part, as expressed by eq 2b. Here the angular brackets denote the ensemble average over all molecular orientations. To measure the sine and cosine part, it is necessary to measure on-resonance, which requires determination of the average frequency of the spectrum. Since we need to compare spin echo decay curves of molecules with different anisotropies δ, it is advantageous to use the dimensionless parameter $\sigma_t \equiv t_p\delta$. σ_t determines the sensitivity of the NMR signal to reorientations during t_m. When $\sigma_t < 1$, eq 2b reduces to $F_{2,\sin}(t_p;t_m) = \langle t_p^2\omega(0)\omega(t_m)\rangle$, i.e., the rotational autocorrelation function for $\eta = 0$ (for $\eta > 0$ one obtains the rotational autocorrelation function of a function similar to eq 1, which, however, has no influence on the determination of the rotational dynamics[22]). For $\sigma_t \gg 1$ the maximum sensitivity to small orientational changes is reached. Under this condition nearly all jumps result in loss of rotational correlation. When data are available over a wide range of σ_t values, detailed information about the molecular jump mechanism can be obtained.[3]

$$F_{2,\cos}(t_p;t_m) = \langle\cos[\omega(0)t_p]\cos[\omega(t_m)t_p]\rangle \qquad (2a)$$

$$F_{2,\sin}(t_p;t_m) = \langle\sin[\omega(0)t_p]\sin[\omega(t_m)t_p]\rangle \qquad (2b)$$

Equation 2 ignores relaxation effects. In reality, the signal dependence is more appropriately described by

$$F(t_m,t_p) = F_2(t_m;t_p)e^{-t_m/T_1}e^{-2t_p/T_2}R_{SD} \qquad (3)$$

Here T_1 denotes the spin−lattice relaxation time, which restores the longitudinal magnetization to its original value. R_{SD} is the relaxation due to spin diffusion caused by local exchange of magnetization,[23] thereby accelerating the return to the original equilibrium. R_{SD} depends on the gyromagnetic ratio, γ, and the inverse square of the distance between observed nuclei.[17] For this reason the enrichment with ^{13}C was limited to 20%. Higher concentrations lead to faster spin diffusion decays, which limit determination of F_2 at lower temperatures. Lower concentrations, of course, reduce the signal-to-noise ratio, which necessitates longer measurement times. It should furthermore be noted that for eq 3 it is assumed that T_2 relaxation does not seriously affect F_2. In our simulations described further below we have simulated the random phase coherence loss, which results in T_2 relaxation in order to check the validity of eq 3. ^{1}H as well as ^{13}C T_1 relaxation times are in excess of 10 s, close to T_g. In combination with the tendency of glucose to slowly crystallize, these long relaxation times exclude excessive averaging.

For these experiments we used a 0.75 g mixture of normal anhydrous α-D-glucose (Merck) crystals and α-D-glucose-*1-^{13}C* or α-D-glucose-*6-^{13}C* (Isotec >99% enriched), such that the total enrichment was around 20%. These already dry mixtures were put in a vacuum oven at 80 °C for at least 2 days to further reduce the total water content. The crystals were placed in an 8 mm NMR tube and heated to 154 °C for about 10 min in an oil bath to melt them and then crash-cooled using tap water to below the calorimetric glass transition temperature T_g of 35 °C. This resulted in a milky glucose glass, which was then sealed in the NMR tube. No effort was made to remove the air bubbles in the glass, since this NMR technique is not sensitive to the presence of these air bubbles. Since the superviscous state of glucose melts is unstable, it is necessary to remelt and crash-cool the samples every 3 days to minimize detrimental effects by crystallization. Crystals can be observed as a structural change of the milky-like glass, but by sticking to this procedure none could be visibly observed in our case. The number of times the sample can be remelted is limited because the melting temperature is close to the caramelization temperature, at which temperature polymerization and conversion to 1,6-anhydroglucose[24] starts and is accompanied by some slight browning of the sample. NMR results of somewhat brownish samples were not significantly different from white samples, however. Another, unwelcome complication when melting glucose crystals

is the enantiomerization of α-glucose into β-glucose. Although this is a slow process, the percentage of β-glucose will increase when the sugar is melted at a high temperature until a 44/56[25] α/β ratio is reached. This becomes problematic for the C-1 enriched glucose since the α and β form have different static chemical shift spectra with different η and δ. For β-glucose the NMR spectra are unknown to us, but comparison of the spectra of the glass with the mixture and the pure α-glucose crystals shows that these parameters are rather similar.

All experiments reported here were carried out on an MSL 300 (Bruker) operating at a ^{13}C frequency of 75 MHz at the Max Planck Institute for Polymer Research in Mainz, Germany.

B. Computer Simulations. To determine the reorientation mechanism, e.g., limited random jump, site specific jumps or rotational diffusion, the (average) jump angle and the jump rate distribution, it is necessary to compare the experimental results with computer simulations. Although similar simulations have been described before,[3] a short description of our version is given below.

The ring of the glucose molecule is represented by a vector that can be rotated along a sphere by Euler transformations around two perpendicular axes, thereby simulating molecular jumps or rotations. The jump probability for the vector is randomly chosen from a predetermined log−Gauss distribution. The vector can be rotated using fixed angles or a given distribution of jump angles. Additionally, a second independent jump process with a different jump angle distribution and jump probability can be added, resulting in a bimodal jump model. For 4000 time steps the molecular orientation is manipulated and selectively stored at 200 time intervals. These orientations are subsequently converted into frequencies using eq 1, and after multiplication with t_p, the sine and cosine parts of the phases of the magnetization vector are stored. This procedure is repeated, typically 10 000 times, and the results are integrated, resulting in a 2D data set with approximately 200 × 80 (t_m,t_p) data points. Before the multiplication with t_p, the phase of the magnetization vector can be changed by rotating this vector over a small angle, randomly chosen from a Gaussian distribution with a width inversely proportional to T_2. In case the NMR results are simulated, the width of the Gaussian distribution is chosen such that a T_2 between 2 and 4 ms results. For each t_p value, the simulated decay curve is fitted to a stretched exponential including a variable baseline

$$F(t) = A_{bs} + A_2 e^{[-(t/\tau)^{\beta}]} \tag{4}$$

The value for the average decay rate or correlation time can be calculated via

$$\langle\tau\rangle = \frac{\tau}{\beta}\Gamma\left[\frac{1}{\beta}\right] \tag{5}$$

For $\sigma_t < 1$, one thus obtains the average rotational correlation time, denoted $\langle\tau_c\rangle$. Note that for small step diffusional rotational dynamics $\langle\tau\rangle/\langle\tau_c\rangle$ decreases with increasing σ_t, whereas this ratio becomes independent of σ_t for random jumps by arbitrary angles.

Results

For a typical spin echo decay experiment 16 t_m values ranging between 100 μs and 5−25 s on a logarithmic scale were acquired. The values of t_m were chosen such that neither the beginning nor the baseline at the end was excessively sampled. This necessitated adaptation of the t_m values when t_p was changed.

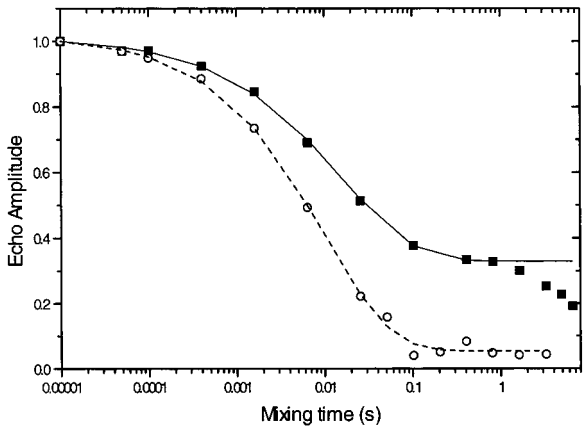

Figure 3. Normalized 2D echo decay curves obtained at $T_g + 9$ K of the cosine part of the signal: (■) $t_p = 200$ μs; (○) $t_p = 500$ μs. For the fits, solid and dashed line, the data were first corrected for spin diffusion decay.

When a cosine data set is acquired using low σ_t values, the resulting curve reaches a plateau at intermediate t_m values, the value of which depending on σ_t. This is clearly shown in Figure 3, where the upper curve (solid squares) represents a normalized cosine data set at $T = T_g + 9$ K with $t_p = 250$ μs ($\sigma_t = 4.40$). For such relative low σ_t values the spins cannot sufficiently evolve under the chemical shift tensor, which puts a limit on the maximal attainable signal decrease as governed by eq 2. As is evident from Figure 3, for long t_m the echo signal decreases further with t_m after having reached this plateau. This decay is caused by spin diffusion, with a decay constant of roughly 25 s, this value being slightly t_p dependent. Because of spin diffusion, it is necessary either to disregard those data points of the cosine data set that have been sampled with a t_m bigger than 6 s or to deconvolute the decay curve with the spin diffusion decay curve where R_{SD} was approximated by an exponential $e^{-t/T_{SD}}$. Both procedures have been used and yield similar results. The lower curve in Figure 3 (open circles) shows a normalized cosine data set with $t_p = 500$ μs ($\sigma_t = 8.80$). The solid and dashed lines in Figure 3 represent fits to eq 4 after deconvolution with R_{SD}.

A small value of t_p results in a large plateau value A_{bs} in combination with a slow decay, thereby enhancing the detrimental effects of spin diffusion. It turned out that cosine data sets (both C-1 and C-6 glucose) acquired with $t_p < 400$ μs could not be adequately fitted due to this reason. The sine data sets acquired for small σ_t are less severely perturbed by spin diffusion, mainly because the baseline of the sine data set is considerable lower (see, e.g., Böhmer et al.[3]). This reflects the fact that sine data sets have small amplitudes for small σ_t whereas cosine data sets start at full amplitude. The sine data sets also allow for the determination of $\langle\tau_c\rangle$.

In Figure 4. $\langle\tau\rangle/\langle\tau_c\rangle$ of glucose enriched at the C-1 position (solid squares) and at the C-6 position (open circles) is plotted vs σ_t for $T_g + 7$ K. The drawn lines represent the computer simulations that best describe the σ_t dependency of $\langle\tau\rangle/\langle\tau_c\rangle$ (solid for the C-1 glucose and dashed for the C-6 glucose) and are discussed further below. Similar plots have been obtained for other temperatures. Typical values for β range between 0.42 and 0.48, with β decreasing with increasing t_p.

To find the (average) jump angle(s), simulated $\langle\tau\rangle/\langle\tau_c\rangle$ versus σ_t curves were generated and compared with the NMR data. In Figure 5 four simulated curves are plotted, each consisting of $\langle\tau(\sin)\rangle$ values for $\sigma_t < 5$ and $\langle\tau(\cos)\rangle$ for larger σ_t values. For specific jump angles (φ) and for some distributions ($K(\varphi)$) (e.g.,

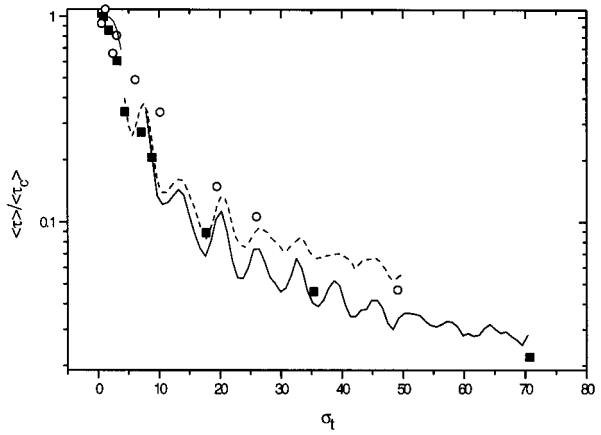

Figure 4. Dependence of the average correlation time, normalized with respect to the average rotational correlation time $\langle\tau_c\rangle$, on σ_t for a superviscous glucose sample with ^{13}C enrichment at the C-1 position (■) and the C-6 position (○) at $T_g + 7$ K. For $\sigma_t < 5$, $\langle\tau(\sin)\rangle$ was used; for $\sigma_t > 5$, $\langle\tau(\cos)\rangle$ was used. The solid line represents a computer simulation for the C-1 glucose; the dashed line, that for the C-6 glucose.

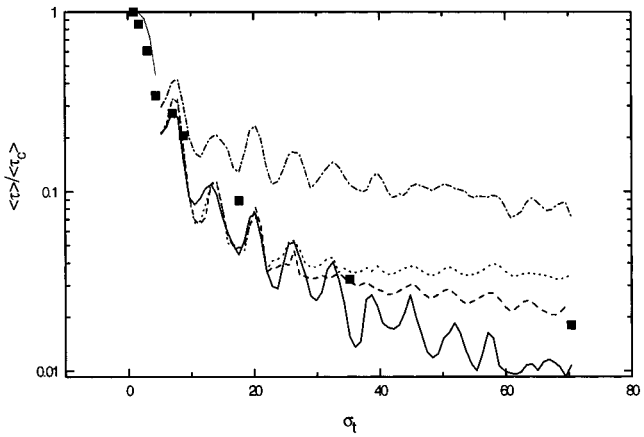

Figure 5. Computer simulations of limited random jump processes. The short-dashed line represents normalized correlation times found for a Gaussian distribution of jump angles with an average of 8°. The long-dashed line represents a process where 75% of the jumps average 1° and 25% average 8°. For the upper trace, the 25% fraction performs 16° jumps, whereas for the lowest, solid trace this fraction performs 4° jumps. For $\sigma_t < 5$, $\langle\tau(\sin)\rangle$ was used; for $\sigma_t > 5$, $\langle\tau(\cos)\rangle$ was used. The solid squares represent $\langle\tau\rangle/\langle\tau_c\rangle$ obtained from NMR data at $T_g + 9$ K.

Gaussian) of jump angles, it has been shown that these curves level off, the plateau of $\langle\tau\rangle$, representing $\langle\tau_j\rangle$ the average jump correlation time, being dependent on the (average) jump angle as given by[9,26]

$$2\tau_j/3\tau_c = \int K(\varphi)\sin^2\varphi\,d\varphi = \langle\sin^2\varphi\rangle \qquad (6)$$

The curve in Figure 5 with the longer dashes shows a simulation with an average jump angle of 8° using a Gaussian distribution of jump angles. However, it is clear from the NMR data (solid black squares) that a plateau is not reached, even for $\sigma_t > 20$. The addition of a second jump process (a 75% fraction with 1−2° jumps) yields a curve that in principle follows the NMR results (Figure 5, dashed line). When T_2 effects are simulated by addition of randomly distributed phases, the curves loose their oscillatory characteristics for large t_p. The two other curves in Figure 5 show the dependence of the curves on different jump angles for the 25% fraction. The upper trace was obtained by simulating 16° jumps, the lowest trace by using 4° jumps. To obtain a reasonable value for β also, it is necessary to use a

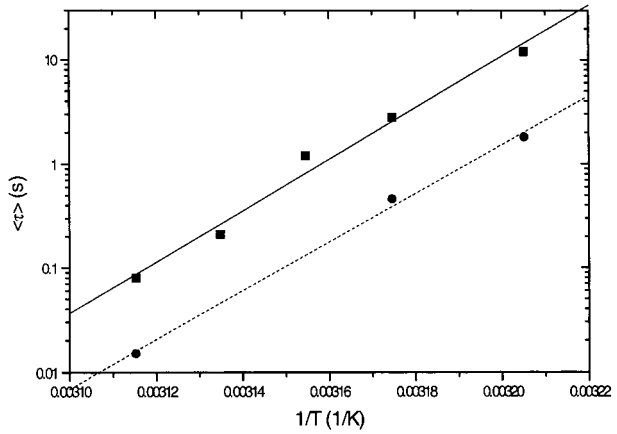

Figure 6. Arrhenius plot of the rotational correlation time of the C-1 glucose (■) and of the correlation for $t_p = 500$ μs of the C-6 glucose (●). Solid and dashed lines show the linear fits though these points.

broad distribution of jump rates, e.g., a log−Gauss distribution. Setting the standard deviation to 1.5 orders of magnitude results in an average β of 0.4−0.5, lying in the same range as the NMR results.

For the C-6 labeled glucose the correlation times are shorter by a factor of 2−3 over the whole σ_t range. Furthermore, the $\langle\tau\rangle/\langle\tau_c\rangle$ ratio is somewhat higher for the C-6 group at intermediate σ_t values than for the C-1 carbon, as is evident from Figure 4. Both observations point toward an increased average jump angle. The higher $\langle\tau\rangle/\langle\tau_c\rangle$ ratio for the C-6 carbon can, in principle, be described by replacing the 25% fraction with an 8° jump angle by an average angle of roughly 12° (compare dashed line with solid line in Figure 4). Values for β were identical to the ones found for the C-1 glucose.

As mentioned before, values for $\langle\tau_c\rangle$ for the C-1 glucose could be determined directly from the sine data sets at low σ_t values and these can be plotted versus $1/T$ in an Arrhenius plot, as is done in Figure 6. From this curve the apparent activation energy, E_{ac}^{app}, can be determined by fitting a straight line through the data points (C-1 glucose: solid squares), yielding an E_{ac}^{app} of 480 ± 40 kJ/mol. Since $\langle\tau_c\rangle$ for the C-6 glucose could not be determined for all three temperatures because of shorter T_1's, $\langle\tau(t_p = 500\mu s)\rangle$ for the C-6 glucose has been plotted in Figure 6 (solid circles) instead. Fitting to a straight line results in a 5% lower activation energy, which, however, is not significant. Additionally, an off-set to shorter (~6 times) correlation times is found since an intermediate value for σ_t was used, causing a 2-fold decrease of $\langle\tau\rangle$, on top of the 2.3-fold lower $\langle\tau_c\rangle$ for the C-6 glucose (1.2 s versus 2.8 s for the C-1 glucose). Plotting $\langle\tau(t_p = 500\mu s)\rangle$ of the C-1 glucose results in a parallel line off-set by a factor of 1.5 due to the difference in δ between C-1 and C-6.

Discussion and Conclusions

In this paper we investigate the geometry and time scale of reorientational processes of superviscous glucose near the T_g of both the main ring and the exocyclic CH_2OH group. It is demonstrated that, by combination of 2D echo decay NMR experiments and Monte Carlo simulations, detailed information on the rotational motion can be obtained for both molecular probes in a limited temperature range above T_g. The average rotational correlation times, as obtained from fitting the 2D spin echo decay curves to eq 4, of the C-1 glucose and the C-6 glucose are similar, 2.8 and 1.2 s respectively, at $T_g + 7$ K, with a nearly identical E_{ac}^{app} of 480 ± 40 kJ/mol. Comparison with the computer simulations show that geometrically the C-1

and C-6 probes have a similar motional pattern; a bimodal, Gaussian, distribution of jump angles of a 75% fraction with 1−2° jumps in combination with 25% fraction with 7−8° jumps and a 75% fraction with 1−2° jumps in combination with a 25% fraction with roughly 12° jumps, respectively. In the following paragraphs factors influencing the accuracy and the reliability of the results are discussed and interpretations of the above results and those of others are presented.

One of the important factors determining the success by which a two-time correlation function can be measured is the length of time beyond which an ensemble remembers its initial position or orientation. The limiting factors for these spin echo decay studies are the T_1 and the T_{SD}. I.e., Deuteron NMR could not be used for the C-6 group since the T_1 was 100 ms at most, which made near T_g studies impossible. Similarly, the ^{13}C T_1 of the C-6 carbon below 315 K prevented the direct determination of $\langle\tau_c\rangle$, although $\langle\tau\rangle$ values for $\sigma_t > 5$ could be used for the determination of E_{ac}^{app}. The ^{13}C T_1 for the C-1 group is long enough to determine slow processes near T_g. At T_g the ^{13}C T_1 is close to 100 s, which is rather long for a glass at its glass transition temperature. From Figure 3, however, it is evident that T_{SD} is short enough to affect the cosine data set, especially since the echo amplitude has stabilized at a relatively high plateau. For higher σ_t values this is less of a problem because of the lower relative amplitude of the plateau and the faster decay rates. Still, values for τ and β were only obtained after the spin echo decay curves were deconvoluted for T_{SD}, or limited to $t_m < 10$ s values.

In principle, $\langle\tau_c\rangle$ can be determined at temperatures lower than presented here, simply by reducing the enrichment. An increase of T_{SD} by a factor of 2 requires the enrichment percentage to be brought down to 7%, which results in an 8-fold increase of measurement time for the same SNR. For t_p values on the order of 2 ms, such measurement would require 3 days, a time over which crystallization may influence the measurements. However, if $\langle\tau_c\rangle$ is the sole parameter of interest, measuring at lower ^{13}C concentrations should allow the measurement of reorientational processes as slow as 50 s. One of the reasons why $\langle\tau_c\rangle$ can be accurately determined is that the sine part of the signal appears less sensitive to T_{SD}. The slowest $\langle\tau\rangle$ that could be reliably determined using cosine data sets was about 2−3 s, whereas a 12 s decay constant could still be measured using a sine data set. As stated above, this can be mostly explained by the fact that the sine data set has a lower baseline.

It is clear that T_1 and T_{SD} relaxations limit the reliability of the fit outcome when σ_t is low and even more so at small $T - T_g$. These decay processes of the longitudinal magnetization result in a standard deviation of $\langle\tau_c\rangle$ and average correlation times above 0.5 s of roughly 40%, whereas for shorter correlation times the standard deviation equals 20%.

The standard deviation for higher σ_t values is lower despite a lower inherent amplitude caused by T_2 relaxation, because the number of averages was increased up to 8 times. This is the main reason the 2D spin echo decay method is better adapted to detect small molecular jumps than 2D exchange spectroscopy since equal sampling over the whole σ_t range favors coarser details. Our glucose samples show a significant disadvantage here, since the relaxation rate (T_2^{-1}) of 400 1/s is relatively large compared to the anisotropy parameter δ of $2\pi \times 2000$ to $2\pi \times 3000$ rad/s. Therefore, no high σ_t values (>80) could be used, which limits the determination of truly fine motional details. Additionally, our simulations show that short T_2 values reduce the oscillations of $F_2(0,t_p)$, $F_2(\infty,t_p)$ and $\langle\tau\rangle$ with increasing σ_t. For $F_2(0,t_p)$ and $F_2(\infty,t_p)$ these oscillations can be calculated analytically by substituting ω in eq 2 by eq 1 and solving the integral (e.g., using Mathematica). Insertion of an additional random phase term (i.e., T_2), which increases with t_p, removes the coherences and causes a smoother decay of $F_2(0,t_p)$ and $F_2(\infty,t_p)$ with t_p. The reduction of the oscillations of $\langle\tau\rangle$ with σ_t (results not shown) is most likely explained by similar arguments.

From the shape of the $\langle\tau\rangle$ vs σ_t plots, it is clear that a plateau is not reached, indicating that either a single jump angle or a Gaussian distribution of jump angles is not a valid model for reorientational motion of glucose or that only small angular jumps occur and that the plateau is not reached yet. However, in the latter case, the average correlation times should be lower for $\sigma_t > 10$, as can be demonstrated by simulations (see lower trace in Figure 5). The curve as measured by NMR is reasonably well described by a bimodal Gaussian distribution of jump angles, a 75% fraction with an average jump angle of 1−2° superimposed on a 25% fraction with an average angle of 7−8°. The bimodal distribution found here is close to the one found by Böhmer et al.[3] for glycerol. They found a large fraction with 2−3° jumps and a smaller, 2−5% fraction with 25° jumps. Furthermore, β values lie in the same range, which indicates that also the distribution of jump rates (e.g., a log−Gauss distribution with a standard deviation of 1.5 decades) is similar. Thus, both glucose and glycerol fit neatly in the polyalcohol group of the classification model as proposed by Böhmer and Angell,[27] even though the molecules themselves appear rather different; i.e., glycerol has more internal motional freedom.

Despite small differences, the data obtained from the C-6 glucose show a rather similar behavior. At 315 K the correlation times for the C-6 glucose are smaller over the complete σ_t range by a factor 2−3. This can be explained by assuming that the average jump angle is larger. The data presented in Figure 4, with an apparently higher plateau for the C-6 glucose support this since such a higher plateau is most likely caused by an increased average jump angle (compare the solid and dashed line in Figure 4 for the C-1 and the C-6 glucose, respectively); e.g., increasing the jump angle of the 25% fraction with larger jumps from 8° to 12° would explain the difference. Since the rotational correlation time is approximately quadratically dependent on the average jump angle for small angular jumps, the above-mentioned difference also explains why $\langle\tau_c\rangle$ of the C-6 glucose is about 2.3 times faster.

The near identical apparent activation energy for the C-6 and C-1 carbons show that the motion of the C-6 group is highly linked to that of the main ring. Most likely a change of orientation of the main ring is followed by the CH_2OH group. Since the CH_2OH group has some additional freedom, it may adjust its relative position after a jump of the ring to minimize its potential energy. E.g., it may rotate further or perform an extra jump to form a stronger H-bridge with a nearby oxygen or proton. The results do not indicate much additional motion and it is therefore unlikely that the above-described motion of the CH_2OH group can be used to explain β-relaxation found at lower temperatures.[7] If the CH_2OH-group rotation were to cause β-relaxation, much shorter rotational correlation times should be present and detectable.

The small differences between C-1 and C-6 rotational mobility seem to be reflected in the spin−lattice relaxation time (T_1(C-1) $\sim 0.2T_1$(C-6)) also. Although one can explain these T_1 differences on the basis of differences in average jump angles and by assuming a broad Cole−Davidson distribution of jump

rates, such an approach is not correct since the activation energy of the T_1 relaxation is 1 order of magnitude smaller than that of the limited random jump process we found here. However, the T_1 relaxation can also be explained by restricted motion on a cone with a high jump rate.[28−31] The activation energy of this librational process of especially the C-6 group (41 kJ/mol), as determined from ^{13}C T_1 measurements, is identical to that of the β-relaxation process, as observed by dielectric relaxation.[7] Possibly, this librational motion of the C-6 group causes the pronounced β-relaxation. Because this type of motion is angularly restricted and is much faster than the α-relaxation in this temperature range (10^{-9}−10^{-8} s compared to 0.001−10 s), it is not picked up by the 2D echo decay technique since the sensitivity for such limited, very fast, motion is too small. A paper with a more elaborate discussion on the T_1 measurements in relation to dielectric relaxation measurements is in preparation.

It is clear from dielectric spectroscopy studies[7] comparing xylose and arabinose on one hand (without CH_2OH group) and glucose and galactose on the other hand that the CH_2OH group significantly influences the β-relaxation process below T_g. This NMR study indicates that it is not a relatively free tumbling of the C-6 group that shows up as β-relaxation but rather a librational type of motion, as suggested by Williams and Watts.[32]

These NMR results show that the changes of rotational motion of glucose with temperature give an estimate of E_{ac}^{app} identical to the E_{ac}^{app} determined by viscosimetry,[33] which suggests that this NMR technique can be reliably used to determine the fragility of a glass. The activation energy determined by dielectric relaxation, on the other hand, is about 30% lower.[7] Partly, this must be caused by frequency differences; i.e., the activation energy as measured by dielectric relaxation was measured at 1 kHz. In our case all frequencies of motion were sampled, and not only subensembles with relaxations rates around 1 kHz. Another factor could be that dielectric relaxation is also sensitive to motion other than rotational motion, e.g., librations.

The study of Böhmer et al.[3] on glycerol shows no difference between different deuterons, because the protons were not site specifically replaced by deuterons. Since the difference between the middle CHOH and outer CH_2OH groups is much smaller than in glucose, a significant difference between the outer and middle hydroxyl groups with regard to time scale and geometry of rotational motion is not anticipated. Still, it would be interesting to see if such a difference exists. It would be highly interesting when other molecules from the monomeric, cyclic carbohydrate group enriched at specific sites become available, which would allow the correlation between molecular motion and molecular shape and other characteristics. The 2D spin echo decay technique would be an excellent technique to study such differences.

From the above experiments and discussion, we conclude that a superviscous, anhydrous glucose melt near T_g behaves like a typical polyalcohol glass with regard to fragility index and the value for β. The high value for E_{ac}^{app} of rotational motion near T_g results from highly cooperative motion that is typical for a glass with a high fragility index. Since both polyalcohols, glucose and glycerol, have similar macroscopic glass characteristics with regard to cooperativity, similarities of other characteristics should not be too surprising. It might well be that not only the distribution of jump rates, reflected in β, are characteristic for glasses with a certain fragility, but also the jump angle distribution. Such a hypothesis, of course, can only be validated if more data on this subject become available. Finally, one can argue that when a side group with characteristics similar to those of a larger submolecular group is present, the local environment it has created and senses is similar to the environment the molecule as a whole senses. Therefore, additional rotational freedom for such a side group need not result in additional motion since the intermolecular forces can be expected to be similar to those controlling the main group motion. Thus, the exocyclic CH_2OH group can be expected to move similarly to the main glucose ring.

Acknowledgment. This study has been carried out with the financial support from the Commission of the European Communities, Agriculture and Fisheries (FAIR) specific RTD program, CT96-1085, *Enhancement of Quality of Food and Related Systems by Control of Molecular Mobility*. It does not necessarily reflect its views and in no way anticipates the Commission's future policy in this area.

References and Notes

(1) Ediger, M. D.; Angell, C. A.; Nagel, S. R. *J. Phys. Chem.* **1996**, *100*, 13200−13212.
(2) Cummins, H. Z.; Li, G.; Hwang, Y. H.; Shen, G. Q.; Du, W. M.; Hernandez, J.; Tao, N. J. *Z. Phys. B−Condens. Mater.* **1997**, *103*, 501−519.
(3) Böhmer, R.; Hinze, G. *J. Chem. Phys.* **1998**, *109*, 241−248.
(4) Fujara, F.; Geil, B.; Sillescu, H.; Fleischer, G. *Z. Phys. B−Condens. Mater.* **1992**, *88*, 195−204.
(5) Ablett, S.; Darke, A. H.; Izzard, M. J.; Lillford, P. J. In *Studies of the glass transition in malto-oligomers*; Blanshard, J. M. V., Lillford, P. J., Eds.; Nothingham University Press: Nothingham, 1993.
(6) Chan, R. K.; Pathmnathan, K.; Johari, G. P. *J. Phys. Chem.* **1986**, *90*, 6358−6362.
(7) Noel, T. R.; Ring, S. G.; White, M. A. *J. Phys. Chem.* **1992**, *96*, 5662−5667.
(8) Noel, T. R.; Parker, R.; Ring, S. G. *Carbohydr. Res.* **1996**, *282*, 193−206.
(9) Hinze, G. *Phys. Rev. E.* **1998**, *57*, 2010−2017.
(10) Hinze, G.; Sillescu, H.; Fujara, F. *Chem. Phys. Lett.* **1995**, *232*, 154−158.
(11) Angell, C. A.; Sare, J. M.; Sare, E. J. *J. Phys. Chem.* **1978**, *82*, 2622.
(12) Böhmer, R.; Ngai, K. L.; Angell, C. A.; Plazek, D. J. *J. Chem. Phys.* **1993**, *99*, 4201−4209.
(13) van den Dries, I. J.; van Dusschoten, D.; Hemminga, M. A. *J. Phys. Chem.* **1998**, *B102*, 10483−10489.
(14) Hinze, G.; Sillescu, H. *J. Chem. Phys.* **1996**, *104*, 314−319.
(15) Böhmer, R.; Hinze, G.; Diezemann, G.; Geil, B.; Sillescu, H. *Europhys. Lett.* **1996**, *36*, 55−60.
(16) Böhmer, R.; Chamberlin, R. V.; Diezemann, G.; Geil, B.; Heuer, A.; Hinze, G.; Kübler, S. C.; Richert, R.; B.; S.; Sillescu, H.; Spiess, H. W.; Tracht, U.; Wilhelm, M. *J. Non-Cryst. Solids* **1998**, *235−237*, 1−9.
(17) Schmidt-Rohr, K.; Spiess, H. W. *Multidimensional solid-state NMR and polymers*; Acadamic Press: London, 1994.
(18) Schmidt-Rohr, K.; Spiess, H. W. *Phys. Rev. Lett.* **1991**, *66*, 3020−3023.
(19) Heuer, A. *Phys. Rev. E* **1997**, *56*, 730−740.
(20) Spiess, H. W. *J. Chem. Phys.* **1980**, *72*, 6755−6761.
(21) Geil, B.; Fujara, F.; Sillescu, H. *J. Magn. Reson.* **1998**, *130*, 18−26.
(22) Wefing, S. Ph.D. Thesis, University of Mainz: Mainz, 1988.
(23) McBrierty, V. J.; Packer, K. J. *Nuclear magnetic resonance in solid polymers*; Cambridge University Press: Cambridge, 1995.
(24) Sugisawa, H.; Edo, H. *J. Food Sci.* **1966**, *31*, 561−566.
(25) Broido, A.; Houminer, Y.; Patai, S. *J. Chem. Soc.* **1966**, *489*, 411−414.
(26) Anderson, J. E. *Faraday Symp. Chem. Soc.* **1972**, *6*, 82−88.
(27) Böhmer, R.; Angell, C. A. Local and global relaxations in glass forming materials. In *Disorder effects on relaxational processes*; Richert, R.; Blumen, A., Eds.; Springer-Verlag: Berlin, 1994.
(28) London, R. E.; Avitabile, J. *J. Am. Chem. Soc.* **1978**, *100*, 7159−7165.
(29) Wittebort, R. J.; Szabo, A. *J. Chem. Phys.* **1978**, *69*, 1722−1736.
(30) Torchia, D. A.; Szabio, A. *J. Magn. Reson.* **1982**, *49*, 107−121.
(31) Schnauss, W.; Fujara, F.; Sillescu, H. *J. Chem. Phys.* **1992**, *97*, 1378−1389.
(32) Williams, G.; Watts, D. C. *Trans. Faraday Soc.* **1971**, *67*, 1971−1979.
(33) Parks, G. S.; Reagh, J. D. *J. Chem. Phys.* **1937**, *5*, 364−367.